Carbohydrate Polymers 313 (2023) 120894

Contents lists available at ScienceDirect

Carbohydrate Polymers

journal homepage: www.elsevier.com/locate/carbpol

Starch-based films doped with porphyrinoid photosensitizers for active skin wound healing

Paloma Lopes [a,b], A. Sofia M. Joaquinito [b], Artur Ribeiro [c,d], Nuno M.M. Moura [b,*], Ana T.P. Gomes [e], Susana G. Guerreiro [f,g,**], M. Amparo F. Faustino [b], Adelaide Almeida [c], Paula Ferreira [a], Manuel A. Coimbra [b], M. Graça P.M.S. Neves [b], Idalina Gonçalves [a,***]

[a] CICECO, Department of Materials and Ceramic Engineering, University of Aveiro, 3810-193 Aveiro, Portugal
[b] LAQV-REQUIMTE, Department of Chemistry, University of Aveiro, 3810-193 Aveiro, Portugal
[c] Centre of Biological Engineering, University of Minho, Campus de Gualtar, 4710-057 Braga, Portugal
[d] LABBELS - Associate Laboratory, Braga, Guimarães, Portugal
[e] CESAM, Department of Biology, University of Aveiro, 3810-193 Aveiro, Portugal
[f] i3S, Instituto de Investigação e Inovação em Saúde, 4200-135 Porto, Portugal
[g] Department of Biomedicine, Biochemistry Unit, Faculty of Medicine University of Porto, 4200-319 Porto, Portugal

ARTICLE INFO

Keywords:
Polysaccharides
Porphyrins
Hydrophobicity
Elasticity
Antimicrobial
Cellular migration

ABSTRACT

Starch is a biodegradable and biocompatible carbohydrate that, when combined with bioactive molecules, can be processed as biomimetic platforms with enhanced performance, allowing its use as active wound dressing materials. Porphyrinoid photosensitizers can tune the physicochemical/functional profile of biomacromolecules, allowing their use in anti-infective strategies. In this work, the feasibility of using the cationic 5,10,15,20-tetrakis (1-methylpyridinium-4-yl)porphyrin tetraiodide (TMPyP) to enhance the physicochemical, mechanical, antimicrobial performance, and wound healing ability of casted starch-based films was studied. TMPyP conferred a reddish coloration to the films, maintaining their pristine transparency. It increased by 87 % the films hydrophobicity and, depending on the TMPyP used, conferred mobility to the starch polymeric chains. Starch/TMPyP-based films effectively photoinactivated *Escherichia coli* (>99.99 %) and favored the wound healing process, even in the absence of light. Therefore, the incorporation of TMPyP into starch-based formulations revealed to be a promising strategy to tune the films compaction degree while giving rise to water tolerant and photosensitive biomaterials that can act as multitarget antimicrobial medical dressings and glycocarriers of active compounds relevant for effective skin wound healing.

1. Introduction

Skin is the largest organ of the human body with the primary function of acting as organism barrier against physical, chemical, and biological assailants (Andreu, Mendoza, Arruebo, & Irusta, 2015; Zhong, Zhang, & Lim, 2010). When its structural and functional integrity is compromised by wounds, the body's endogenous wound healing process immediately begins ensuring the skin's total recovery (Tottoli et al., 2020; Zeng et al., 2018). Medical dressings aim to modify and/or manipulate the wound environment to protect the wound from infections and decrease the wound healing time. Currently, wound dressings take variable forms, including semipermeable films, foams, hydrocolloids, and hydrogels (Andreu et al., 2015; Gupta, Agarwal, & Alam, 2010; Liang, He, & Guo, 2021; Mogoşanu & Grumezescu, 2014; Simões et al., 2018; Zarrintaj et al., 2017). The next generation of wound dressings are being explored as bioactive materials delivering collagen, enzyme debriding or antimicrobial agents, that could modulate the wound healing process, while decreasing the use of external substances to maintain the asepsis, namely antibiotics (Andreu et al., 2015; Mogoşanu & Grumezescu, 2014).

Starch is a natural carbohydrate that has been explored for developing films, hydrogels, hydrocolloids, ointments, and nanofibrous

* Correspondence to: N. Moura, Department of Chemistry, University of Aveiro, 3810-193 Aveiro, Portugal.
** Correspondence to: S. Guerreiro, Department of Biomedicine, Faculty of Medicine of University of Porto, 4200-319 Porto, Portugal.
*** Correspondence to: I. Gonçalves, Department of Materials Engineering and Ceramics, University of Aveiro, 3810-193 Aveiro, Portugal.
E-mail addresses: nmoura@ua.pt (N.M.M. Moura), scgomes@med.up.pt (S.G. Guerreiro), idalina@ua.pt (I. Gonçalves).

https://doi.org/10.1016/j.carbpol.2023.120894
Received 27 November 2022; Received in revised form 21 February 2023; Accepted 6 April 2023
Available online 10 April 2023

scaffolds with potential to be used as wound dressings (Torres, Commeaux, & Troncoso, 2013). It is composed of two polysaccharides, the mainly linear amylose and the highly branched amylopectin, both made of polymeric chains containing D-glucopyranose residues linked by (α1,4) glycosidic bonds and branches through (α1,6) glycosidic bonds (Bertoft, 2017; Feng et al., 2018). Starch is of high value for various industries due to its gelatinization capacity. Apart from its use as a thickener, gelling agent, and glue in industrial applications (Ai & Jane, 2015), starch, due to its easy ability of acquiring thermoplastic properties, has also been explored for the development of biobased plastic films (Ai & Jane, 2015; Hemamalini & Giri Dev, 2018; Liu, Xie, Yu, Chen, & Li, 2009; S. Wang, Li, Copeland, Niu, & Wang, 2015; Zhu & Xie, 2018); and hydrogels (Hassan, Niazi, Hussain, Farrukh, & Ahmad, 2018; Pal, Banthia, & Majumdar, 2006; Zhai, Yoshii, Kume, & Hashim, 2002, Jukola, Nikkola, Gomes, Reis, & Ashammakhi, 2008; Sunthornvarabhas, Chatakanonda, Piyachomkwan, & Sriroth, 2011; H. Wang et al., 2011). Starch-based films are isotropic, odorless, tasteless, colorless, and non-toxic (Ai & Jane, 2015; Laohakunjit & Noomhorm, 2004; Liu et al., 2009). However, they tend to be brittle, due to their highly compacted structure, and very sensitive to moisture conditions, due to the presence of various hydroxyl groups in the polymeric chains. To overcome the high brittleness and hydrophilicity of starch-based materials, the use of chemically modified starch (Lancuški et al., 2017; W. Wang et al., 2016) or starch blended with plasticizers (Laohakunjit & Noomhorm, 2004; Liang & Ludescher, 2015; Liu et al., 2009) or synthetic polymers, such as polyvinyl alcohol (Das, Uppaluri, & Das, 2019; Hassan et al., 2018; H. Wang et al., 2011; Zhai et al., 2002), polylactic acid (Sunthornvarabhas et al., 2011), and polycaprolactone (Jukola et al., 2008), have been considered (Das et al., 2019). Starch-based films *per si* have limited application as active wound dressings, once they have no particular biological properties and can be easily metabolized by bacteria (Ruhl et al., 1994), leading to wound-related infections. The development of new active starch-based dressings as wound treatment systems is now focused on the immobilization of active biomolecules, such as polyphenols (Lopes et al., 2021; Pyla, Kim, Silva, & Jung, 2010) and proteins (Moreno, Atarés, & Chiralt, 2015), with antioxidant, anti-inflammatory, and/or antimicrobial properties. For instance, *Escherichia coli(E. coli)* O157:H7 cells were inactivated in 5–7 log CFU/mL by starch-based films impregnated with fresh and thermally processed tannic acid (Pyla et al., 2010); *Staphylococcus aureus (S. aureus)* growth was inhibited by starch-based films coated with essential oils, showing zones of inhibition ranging from 9 mm to 24 mm diameter (Kuorwel, Cran, Sonneveld, Miltz, & Bigger, 2011); starch-based films blended with hyaluronic acid and an ethanolic extract of propolis exhibited antibacterial activity against *S. aureus* (inhibition zone diameter of 2.08 ± 0.14 mm), *E. coli* (inhibition zone diameter of 2.64 ± 0.18 mm), and *Staphylococcus epidermidis* (inhibition zone diameter of 1.02 ± 0.15 mm) (Eskandarinia et al., 2019). Nevertheless, their contribution to cell migration during wound healing remains unexplored.

Antimicrobial photodynamic therapy (aPDT) has emerged in recent years as an alternative therapeutic technique to the conventional antimicrobial treatment of various infections by bacteria, fungi, and viruses, including drug-resistant microorganisms and those that form biofilms (Mesquita, Dias, Neves, Almeida, & Faustino, 2018; Vallejo et al., 2021). This methodology requires the activation of a photosensitizer (PS) by irradiation with a specific visible light wavelength in the presence of dioxygen ($^3O_2$), giving rise to reactive oxygen species (ROS), mainly singlet oxygen ($^1O_2$). ROS oxidize different biomolecules of the microorganisms' external structure and genetic material, such as lipids and proteins, causing irreparable biological damages and consequent microbial photoinactivation (Kwiatkowski et al., 2018; Mesquita, Dias, Neves, et al., 2018; Nyman & Hynninen, 2004; O'Connor, Gallagher, & Byrne, 2009; Vallejo, Moura, Faustino, et al., 2021; Zhang et al., 2018). On the other hand, these species can also trigger the skin wound regenerative process through the immune system response to the wound-site, inducing new tissue growth and neoangiogenesis (Vallejo et al., 2021; Vallejo, Moura, Faustino, et al., 2021). Additionally, since $^1O_2$ and free radicals can interact with microbial structures and metabolic pathways in microorganisms (Hanakova et al., 2014), the non-specificity of ROS action avoids the microbial resistance to aPDT (Costa et al., 2011; Tavares et al., 2010; Vieira et al., 2018). Among all the classes of photosensitizing compounds, porphyrins are one of the most studied for aPDT application. These aromatic tetrapyrrolic macrocycles with a highly conjugated system show characteristic ultraviolet-visible absorption spectra: an intense Soret band at *ca.* 400 nm region accompanied by a series of Q bands of lower intensity in the 500–700 nm region (Kadish, Smith, & Guilard, 2010). Porphyrins are recognized to have adequate physicochemical characteristics for different therapeutic applications due to their low toxicity in the absence of irradiation. In addition, they do not produce toxic metabolites or cause mutagenesis in microorganisms, and may also help in clinical diagnosis due to their ability to emit fluorescence (Berg et al., 2005; Kwiatkowski et al., 2018; Mesquita, Dias, Neves, et al., 2018; O'Connor et al., 2009). Some of these features are particularly relevant in their actuation as photosensitizers in aPDT and consequently to deal with the growth of antibiotic resistance problematic. Although the PS production cost can compromise the aPDT massification, its immobilization onto inert solid supports allowing its recovery, reuse, and recycling, is turning aPDT economically viable and environmentally friendly (Alves et al., 2014; Carvalho et al., 2010; Mesquita et al., 2014). To this extent, different supports like nanoparticles (organic, inorganic, and hybrids), liposomes and derivatives, nanogels and nanofibers, films, biopolymers, and carbon nanotubes have been used to immobilize porphyrins, allowing to concomitantly tune the supports physicochemical, mechanical, and biological performance (Gomes, Neves, & Cavaleiro, 2018; Jiang, Gan, Gao, & Loh, 2016; Mesquita et al., 2018; Mesquita, Dias, Neves, et al., 2018). At an end-use stage, some of the non-biodegradable and non-biocompatible materials are still forwarded to incineration. However, supports based on polysaccharides with biodegradability, biocompatibility, and the possibility to be absorbed by the human body can be considered excellent alternatives to develop new delivery biobased systems for PS with zero-waste and have not been explored yet.

In this work, it is hypothesized that starch-based films doped with porphyrins can be used for developing antimicrobial biomaterials and glycocarriers of bioactive molecules suitable to enhance the skin wound healing process. The influence of cationic 5,10,15,20-tetrakis(1-methylpyridinium-4-yl)porphyrin tetraiodide, a highly efficient photosensitizer, on chromatic, physicochemical, mechanical, photophysical, antimicrobial, and wound healing properties of starch-based films was evaluated.

2. Material and methods

Starch (70 % amylopectin (350 kDa) and 30 % amylose (50 kDa), (Gonçalves et al., 2020)) was recovered from potato washing slurries supplied by A Saloinha, Lda, a Portuguese potato chips industry. Glycerol was provided by LabChem (Lisbon, Portugal). 5,10,15,20-tetrakis (1-methylpyridinium-4-yl)porphyrin (TMPyP) was synthesized by reacting the corresponding neutral form, 5,10,15,20-tetrakis(pyridin-4-yl)porphyrin (TPyP) with methyl iodide, as described in the literature (C. Simões et al., 2016; Vallejo et al., 2021) and the purity checked by chromatographic and ^{1}H NMR techniques. The n-octanol:water partition coefficient of TMPyP (miLog P = −6.37) was evaluated using the MolinspirationWebME Editor 3.81, http://www.molinspiration.com (accessed February 2023). Dulbecco's modified Eagle's medium (DMEM, Invitrogen Life Technologies, Paisley, UK), 10 % fetal bovine serum (FBS, Invitrogen Life Technologies, Paisley, UK), 1 % penicillin/streptomycin (Invitrogen Life Technologies, Paisley, UK), Roswell Park Memorial Institute 1640 medium (RPMI, Invitrogen Life Technologies, Paisley, UK) were obtained for the wound healing assay. All the purchased chemicals were of analytical grade.

2.1. Preparation of starch/TMPyP-based films

Starch- and starch/TMPyP-based films were prepared by solvent casting, adapting a reported procedure (Gonçalves et al., 2020). Dispersions of starch (4 % *w/V*), glycerol (30 % *w*/w related to the starch dry weight), the plasticizer, and different TMPyP concentrations (0.25 %, 0.50 %, and 0.75 % w/w related to the starch dry weight) were prepared in distilled water, heated at 95 °C, and stirred for 30 min with constant magnetic stirring (200 rpm). Each gelatinized starch- and starch/TMPyP-based dispersion was degassed using a vacuum pump (Vacuum Pump V-300, Buchi, Maia, Portugal), transferred (21.0 ± 1.0 g) to plexiglass molds (12 cm × 12 cm), and dried at 25 °C for 12 h. Afterwards, the resulting films were pulled out from the molds and stored for 20 days at room temperature (20 °C ± 5 °C) in a chamber with 50 % ± 5 % relative humidity controlled using a saturated magnesium nitrate solution prior characterization. Films without TMPyP were prepared and used as control.

2.2. Characterization of starch/TMPyP-based films

2.2.1. Chromatic properties

Chromatic parameters were determined through CIELAB colour scale analysis using a Chroma meter CR-400 colorimeter (Konica Minolta Sensing, Inc., Lisbon, Portugal) in indirect natural luminosity conditions (Gonçalves et al., 2020). Samples were analyzed in triplicate.

2.2.2. Traction resistance

To determine the film's traction resistance, strips (7 cm × 1 cm) were cut, and their thickness was measured using a Mitutoyo micrometer (EACAMPOS, Porto, Portugal) in 3 to 5 different parts of the sample. The mechanical properties analysis was performed at room temperature (20 °C ± 5 °C), at 50 % ± 5 % relative humidity, through stress tests using a TA.XTplusC texture analyzer (Stable Micro Systems, Godalming, United Kingdom) equipped with miniature traction claws (A/MTG). The test was performed at a speed of 0.5 mm/s and with a return distance of 50 mm. Mechanical parameters, such as the Young's modulus, tensile strength, and elongation at break were determined based on the tension-deformation curves obtained (expressed in strength, N, by distance, mm) (Gonçalves et al., 2020). At least 6 replicates of each film were analyzed.

2.2.3. Wettability and water solubility

The films wettability was determined by measuring the contact angle performed between a water drop and the film surfaces using an OCA 20 instrument (Dataphysics, Porto, Portugal). The films water solubility was determined by weight loss percentage after water immersion, following described methodologies (Basiak, Lenart, & Debeaufort, 2018; Nunes et al., 2013).

2.2.4. Release of TMPyP in aqueous medium and PBS

The efficiency of starch-based films to act as TMPyP glycocarriers was evaluated through the TMPyP release from the polymeric matrix to the surrounding aqueous media. Squares (2 cm × 2 cm) of each developed film were immersed in distilled water containing sodium azide (0.02 % *w/V*) and stirred at room temperature for 7 days. Afterward, 300 μL of each residual aqueous solution was transferred into 96-wells sterile plates (Deltalab, Barcelona, Spain) and the corresponding absorbance spectra between 380 nm to 480 nm were obtained. Each absorbance measurement was carried out in triplicate. The calculation of TMPyP release percentage was made based on the Beer-Lambert law, considering the molar absorptivity (ε) of TMPyP solubilized in distilled water containing sodium azide (0.02 % *w/V*) of 116,554 L mol^{-1} cm^{-1}, and an optical path length (l) of 0.686 cm based on information provided by the manufacturer for the aqueous solution volume used (300 μL).

2.2.5. Ex vivo TMPyP skin permeation studies

The *ex vivo* permeation through pig abdominal skin of TMPyP entrapped in starch-based films was evaluated using Franz diffusion cells (V-Series Stirrers for Franz Cells; PermeGear, Hellertown, PA, USA) system with a diffusion area of 0.64 cm^2. The pig skin was selected as a model for human skin permeability since it presents properties like barrier thickness and follicular structure that resemble human skin (Barbero & Frasch, 2009; Ferreira & Ribeiro, 2015). Fresh abdominal porcine skin was collected from a local slaughterhouse and the subcutaneous fat was removed using surgical scissors. Pig skin samples were washed with phosphate-buffered saline (PBS, pH 7.4) and the samples integrity was checked out with a portable magnifying lamp. The pig skin sections were placed in the Franz diffusion cells with the dermis facing the receptor compartment and the films were placed on the top of the skin. Prior to the permeation studies, each developed film was weighted and kept on a desiccator protected from light for 24 h. Pig skin and starch- and starch/TMPyP-based films were fixed between the receptor and the donor compartments, and the receptor compartment was filled with 5.0 mL sodium lauryl sulfate (16 mM) micellar solution. To provide a skin surface of 32 °C by heat dissipation, the micellar solution was continuously stirred and thermostatized at 37 °C through a circulating water bath (Ouitas & Heard, 2009). Aliquots were taken at specific time points (1 h, 2 h, 4 h, 8 h, and 24 h) and the same volume was replaced with micellar solution. Absorbance of each collected aliquot was measured at 430 nm wavelength and the TMPyP amount was quantified against a calibration curve ($y = 0.7138\times - 0.7777$, $r^2 = 0.9895$) prepared using increasing concentrations of TMPyP (0.0 μM, 2.0 μM, 5.0 μM, 10 μM, 20 μM, and 30 μM). The measurements were recorded in triplicate using a microplate Synergy MX spectrofluorometer (BioTek, Lisbon, Portugal) equipped with a temperature controller. At the permeation experiments end, starch/TMPyP-based films were collected, stored in a desiccator protected from light for 24 h, and further weighted. The film weight loss percentage was determined according to Eq. (1):

$$\text{Weight}_{\text{loss}}(\%) = \frac{W_i - W_f}{W_f} \times 100 \quad (1)$$

where W_i and W_f corresponds to the film's initial and final weight, respectively. To determine the TMPyP amount that migrates onto the pig skin surface, the skin samples were collected, sliced, immersed in DMSO for 4 h with constant stirring (200 rpm), and the concentration of TMPyP migrated onto the pig surface was spectrophotometrically obtained using the aforementioned calibration curve. The TMPyP amount that remained in the pig skin sections was calculated according to Eq. (2):

$$\text{TMPyP}_{\text{in\_skin}}(\%) = \text{TMPyP}_i - \left(\text{TMPyP}_f + \text{TMPyP}_r\right) \quad (2)$$

where TMPyP_i and TMPyP_f correspond to the amount of TMPyP in starch/TMPyP-based films before and after permeation, respectively, and TMPyP_r corresponds to the TMPyP amount that permeated the pig skin. To determine the TMPyP amount that remained entrapped into the starch-based polymeric matrices, the films were immersed in DMSO, stirred until complete dissolution, and the TMPyP concentration was spectrophotometrically obtained as previously described. *Ex vivo* TMPyP skin permeation studies were performed in triplicate.

2.2.6. Singlet oxygen generation

The photochemical ability of starch/TMPyP-based films to generate singlet oxygen ($^1O_2$) was evaluated by measuring the absorption decay of 1,3-diphenylbenzofuran (DPiBF) at 415 nm, selected as the $^1O_2$ quencher (Spiller et al., 1998). Each film was cut in strips of equal mass (28.5 mg), immersed into 3 mL *N,N*-dimethylformamide (DMF) and then kept at room temperature for 30 min protected from light. After this period, 50 μM of DPiBF was added to each film container and the initial DPiBF absorbance value at 415 nm was registered using a UV-2501PC spectrophotometer (Shimadzu, Kyoto, Japan). Each sample was irradiated with red light LEDs (630 nm ± 20 nm, 14 mW/cm^2) at room temperature under magnetic stirring (50 rpm) and the DPiBF absorption

decay, due to the singlet oxygen production, was measured after 15 min and 30 min of light irradiation. Singlet oxygen production measurements were performed in duplicate for each developed starch/TMPyP-based material using DPiBF as control.

2.2.7. Antimicrobial photodynamic properties

The antimicrobial ability of starch/TMPyP-based films was determined by monitoring the bioluminescence of an *E. coli* (Top 10, Invitrogen, USA), previously transformed (Alves et al., 2008), in a 20/20 GloMax® luminometer (Promega Corporation, Madison, Wisconsin). Since the viability of this bacterium is related with its bioluminescence, this allows to evaluate, in real-time, the aPDT efficiency of the starch/TMPyP-based films. The strong correlation between the colony-forming units (CFU) and the bioluminescent signal of the bioluminescent *E. coli* used in this work has already been proved and described (Alves et al., 2008). Thus, an overnight growth culture of bioluminescent *E. coli* culture was tenfold diluted in phosphate-buffered saline (PBS), pH 7.4, to a final bioluminescence of 10^7 relative light units (RLU) (corresponding to a concentration of $\approx 10^7$ CFU/mL). The obtained suspension was equally distributed (10 mL) in the wells of a six wells plate. Then, films containing the lowest and the highest TMPyP concentrations were cut as thin strips to add 20 μM of TMPyP into the wells. The following controls were included in the assays: i) light control (LC) - comprising just the bacterial suspension submitted to the same irradiation of the aPDT protocol; ii) 0.00 % TMPyP control - comprising bacterial suspension and starch-based films without TMPyP and submitted to the same light irradiation of the aPDT assays; iii) dark control (DC) - comprising the bacterial suspension and the starch/TMPyP-based films (0.25 % TMPyP or 0.75 % TMPyP corresponding to 20 μM TMPyP) protected from light. All the bacterial suspensions were incubated in the presence of starch/TMPyP-based films in the dark under magnetic stirring for 30 min. Afterward, the light control, the neat starch-based film 0.00 % TMPyP, and the films containing 0.25 % TMPyP and 0.75 % TMPyP were irradiated with white light delivered by a commercial LED system at an irradiance of 25 mW/cm^2, measured with a power and Coherent FieldMaxII-Top energy meter connected to a high-sensitivity PS19Q sensor (Coherent, Saxonburg, PA, USA), for a minimum period of 30 min. Aliquots of 1.0 mL were removed from each well at constant intervals of 5 and 10 min for bioluminescence measurement using the 20/20 GloMax® luminometer (Promega Corporation, Madison, Wisconsin). For the quantification of colony-forming units per mL (CFU mL^1), several dilutions (from 10^{-1} to 10^{-5} of the initial concentration) of the collected aliquots at times 0 min and 30 min were pour plated in trypticase soy agar (TSA). The plates were incubated at 37 °C for 18 h, and then the obtained colonies were counted. Two independent tests were carried out and the results were averaged. Furthermore, TMPyP release from starch-based films to PBS was also assessed using the method described in Section 2.2.4.

2.2.8. Wound healing in vitro assay

For the wound healing assay, skin human microvascular endothelial cells (HMEC, ATCC) and skin human dermal fibroblasts (HDF, ATCC) were used. HMEC were cultured in Roswell Park Memorial Institute 1640 medium supplemented with 10 % FBS and 1 % penicillin/streptomycin. HDF were cultured in Dulbecco's modified Eagle's medium, supplemented with 10 % fetal bovine serum and 1 % penicillin/streptomycin. Cell cultures were used at 8–12 and 20–24 passages for HMEC and HDF, respectively, and maintained in a humidified atmosphere containing 5 % CO_2 at 37 °C. HDF and HMEC were allowed to grow until 70–80 % confluence. For sub-culturing attached cells, the old medium was removed from the plate and the cells were washed out with PBS solution and 1.0 mL of trypsin was added. After 1 min, trypsin was removed, and the plate was incubated for 5 min at 37 °C. Complete medium for the respective cell type was added and cells were counted using a Double Neubauer Ruled Metallized Counting Chamber. For the wound healing experiment, the ibidi® culture-insert 2-well for gap formation was used in a 24 well culture plate, according to the manufactured. A suspension of cells with density of 5×10^5 cells mL^{-1} was prepared and 70 μL were added to each well of the culture-insert chamber and incubated for 24 h in a humidified atmosphere at 37 °C (5 % CO_2). The insert was removed, the cells were washed with PBS to remove cell debris. Then, 200 μL of cell culture medium was added to each well with the respectively treatment. Treatment samples were previously prepared: starch- and starch/TMPyP-based films (0.25 %, 0.50 %, and 0.75 % TMPyP *w*/w related to the starch dry weight) were cut using a 6 mm punch to obtain 28.27 mm^2 discs, different portion of the discs were added and incubated under dark conditions at 37 °C for 30 min. Control group only had complete cellular medium. For PDT-assisted experiments, one plate was irradiated with a red-light LED lamp (652 nm at an irradiance of 5.0 mW cm^{-2}) for 15 min, corresponding to 4.5 J cm^2 while the other one was kept in the dark. Afterward, both plates were incubated in a humidified atmosphere at 37 °C (5 % CO_2) for 24 h. The light irradiance was measured with a power and Coherent FieldMaxII-Top energy meter connected to a high-sensitivity PS19Q sensor (Coherent, Saxonburg, PA, USA). Pictures of the gaps were taken at time point 0 and after 24 h, using an inverted microscope (Nikon, TMS-F model) with D40X Nikon camera. The experiments were performed in triplicate ($n = 3$). Wound closure was measured by gap area using the Java-based software program Image J.

2.2.9. Statistical analysis

A *t*-test was performed with equal variances and a 0.05 *p*-value using the Microsoft Excel 2018 software to analyze the statistical significance of data obtained in all the performed starch- and starch/TMPyP-based films characterization tests. Significance between the different samples was represented in the form of lowercase letters. The significance of bacterial viability between treatments, and along the experiments, was assessed by two-way ANOVA analysis of variance. Tukey's multiple comparison test was used for a pairwise comparison of the means. For different treatments, the significance of differences was evaluated by comparing the results obtained in the test samples with each other and with the results obtained for the correspondent control samples, for the different times. A value of $p < 0.05$ was considered significant. Two independent experiments were conducted in duplicate for each assay. For the *in vitro* wound healing assay statistical analysis of the obtained data was carried out by GraphPad Prism® 7.04 (GraphPad Software, CA, USA), using a one-way analysis of variance (ANOVA), with a Tukey test for multiple comparisons. A $p < 0.05$ of the mean comparison between the groups and against the non-irradiated cell control was considered as statistically significant in each experiment.

3. Results and discussion

Starch-based films containing different percentages (0.00 %, 0.25 %, 0.50 %, and 0.75 % w/w related to the starch dry weight) of the cationic 5,10,15,20-tetrakis(1-methylpyridinium-4-yl)porphyrin tetraiodide (TMPyP) were prepared by solvent casting method, characterized, and tested on wound healing as described below.

3.1. Physical and mechanical characterization of starch/TMPyP-based films

The characterization of starch/TMPyP-based films referred as 0.25 % TMPyP, 0.50%TMPyP, and 0.75 % TMPyP showed that TMPyP amount affected the physical and mechanical features of the starch-based film, when compared with the material without porphyrin (0.00 % TMPyP). From a chromatic point of view (Fig. 1), TMPyP decreased the lightness (L^*) values from 92 to 57 and increased the red-green (a^*) coordinate values from 0.50 to 28 of starch-based films (Fig. 1A), thus conferring them a reddish coloration while maintaining their characteristic transparency (Fig. 1B). These chromatic changes varied linearly with the TMPyP concentration and were caused by the pristine intense red

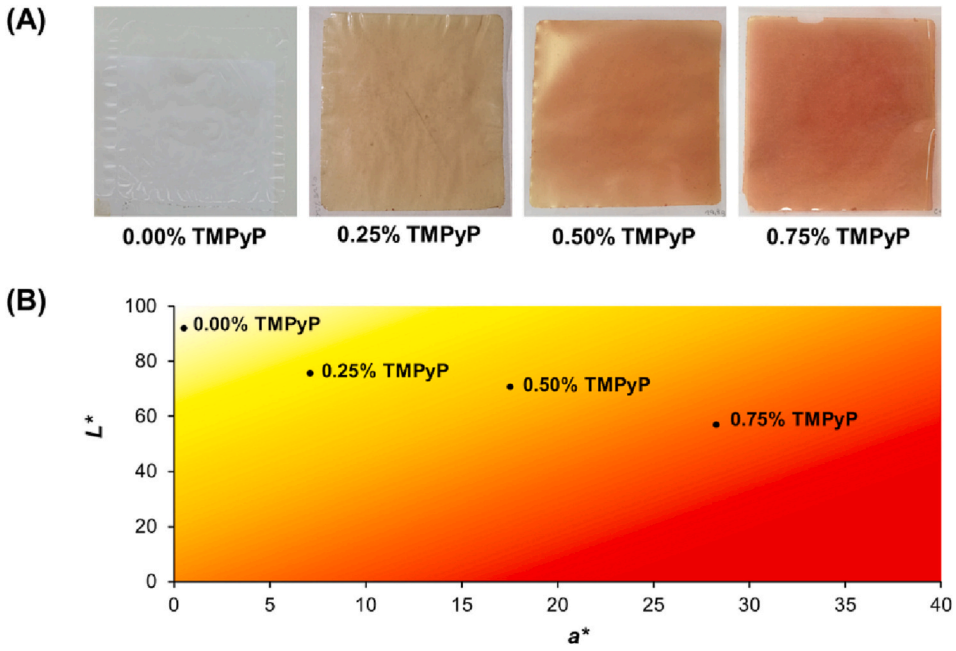

Fig. 1. Chromatic properties of starch- and starch/TMPyP-based films: (A) digital images and (B) lightness (L^*) and red-green (a^*) coordinate values.

coloration of TMPyP. Moreover, no aggregates formation at the bio-based polymer surface was noticed upon the addition of TMPyP, even in the starch-based film doped with the higher concentration of PS. The lack of TMPyP aggregates and the good uniformity/consistence of the films prepared show good compatibility between TMPyP and the support structure, affording starch/TMPyP-based films with appropriate features to generate ROS, mainly singlet oxygen, and to be used as photosensitizer materials in wound healing.

Regarding the influence of TMPyP concentration on the thickness and traction properties of starch-based films (Fig. 2), 0.25 % and 0.50 % TMPyP originated thinner films than the neat ones, decreasing their thickness from 74 μm to 60 μm (Fig. 2A). In contrast, 0.75 % TMPyP did not significantly change the thickness of the films, although still presenting a slightly lower thickness value than the control sample. As the same weight of gelatinized starch- and starch/TMPyP-based dispersions was used in the solvent casting process, the films thickness decrease resulted from the starch/glycerol ratio change promoted by the TMPyP incorporation which influences the intermolecular molecular bonding between starch, glycerol, and TMPyP molecules and, therefore, the subsequent molecular rearrangement. On the other hand, the highest

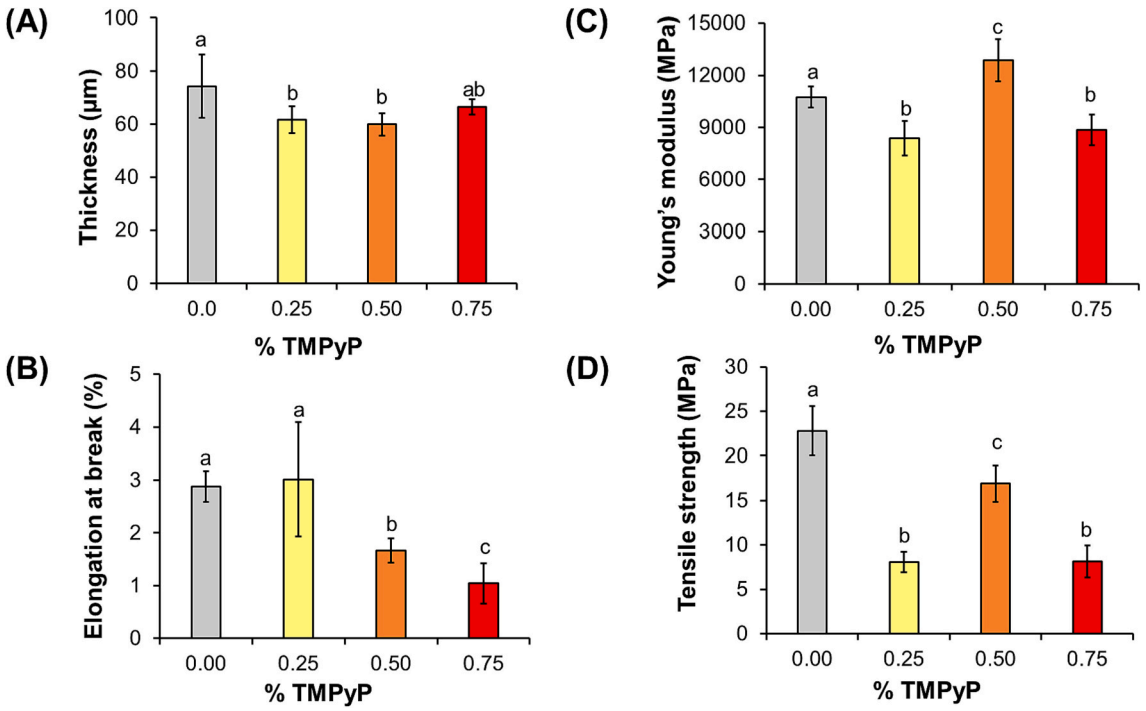

Fig. 2. Traction performance of starch- and starch/TMPyP-based films: (A) Thickness; (B) elongation at break; (C) Young's modulus; and (D) tensile strength. (For statistic difference analysis, lower-case letters were used to highlight the significant differences ($p < 0.05$) between the starch- and starch/TMPyP-based films).

TMPyP concentration difficulted the hydrogen bonding between starch, glycerol, and TMPyP molecules, thus avoiding the films thickness decrease.

After being exposed to a traction force, it was observed that TMPyP concentrations higher than 0.25 % decreased the films elongation at break from 3 % to 1 % (Fig. 2B), thus originating less stretchable materials than the neat materials. On the other hand, when 0.25 % and 0.75 % TMPyP were added into the starch-based formulations, the films Young's modulus decreased from 10,740 MPa to 8360 MPa and 8850 MPa, respectively (Fig. 2C), thus increasing the films elasticity. For 0.50 % TMPyP, the films Young's modulus changed oppositely, increasing from 10,740 MPa to 12,860 MPa, thus becoming more rigid than the control films. Furthermore, TMPyP decreased the films tensile strength from 23 MPa to 8 MPa (Fig. 2D), although with minor impact for films containing 0.50 % TMPyP (17 MPa), thus decreasing the traction resistance of the neat starch-based films. Therefore, 0.25 % and 0.75 % TMPyP promoted mobility to the starch polymeric chains, while 0.50 % TMPyP increased their rigidity. These mechanical changes may result from the intermolecular bonds that TMPyP established within the starch network and/or other TMPyP molecules (Gonçalves et al., 2021). When added in lower or higher concentrations than 0.50 %, the intermolecular hydrogen bonding between starch polymeric chains can be disrupted by TMPyP molecules, allowing their disentanglement. In turn, for TMPyP concentration around 0.50 %, besides these intermolecular bonds with starch, other interactions between the TMPyP molecules can also take place in the system, promoting the film structure compaction. Similar trend has been reported for glycerol and genipin that within a certain range of concentrations act as a plasticizer, promoting the films extensibility by increasing intermolecular spacing, while for quantities outside this concentrations range compromises the plasticizing effect, inducing the films compaction (Gonçalves et al., 2021; Torres et al., 2013). Thus, the mechanical tuning ability that TMPyP promotes in starch-based films allows to develop biomaterials suitable to manage a wide variety of wound types. Furthermore, the outstanding Young's modulus observed for all the developed starch-based films highlights the networked formed during the starch retrogradation phase, providing films with strength against deformation (Gonçalves et al., 2020; Thakur et al., 2018).

From the wettability point of view (Fig. 3), TMPyP significantly increased water contact angle of the bottom surface (in direct contact with the plexiglass plate during casting) of starch-based films from 39° to 91°, reaching a stationary value for TMPyP concentrations above 0.50 %, thus conferring hydrophobicity to the bottom film's surface. This tendency was also evidenced on the film's top surface (exposed to air during casting), however, the water contact angle just increased up to a 45° - 49° range and, therefore, this film surface remained hydrophilic. Thus, starch/TMPyP-based films showed hydrophobic and hydrophilic surfaces, particularly for TMPyP concentrations higher than 0.25 %. This heterogeneous wettability profile is caused by the different density values of each component (starch, glycerol, water, and TMPyP) that, during solvent casting, originate their distinct distribution over the final material (Gonçalves et al., 2020). When incorporated into the starch-based formulations, TMPyP becomes the most hydrophobic molecule in the system due to the lower amount of polar functional groups than the ones present in starch and glycerol, justifying the water contact angle increase in the bottom surface of each developed film. On the other hand, as glycerol is soluble in water, the solvent used in the films preparation, over the casting, tends to migrate to the top part of the starch-based polymeric matrix, thus contributing for the top film surface hydrophilicity. Furthermore, as a metal complex constituted by a π-conjugated macrocycle (Kuzmin, Chulovskaya, & Parfenyuk, 2018), TMPyP may acquire nonplanar conformation onto the films surface, which might impart roughness and, thus, minimizing their water wettability.

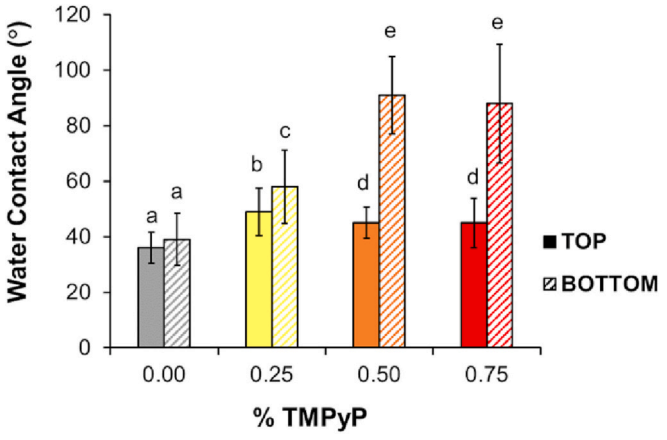

Fig. 3. Water contact angle values of starch- and starch/TMPyP-based films. TOP and BOTTOM are related with the film faces exposed to air and in direct contact with the plexiglass plate during the solvent casting process, respectively. (For statistic difference analysis, lower-case letters were used to highlight the significant differences ($p < 0.05$) between the starch- and starch/TMPyP-based films).

Despite TMPyP increased the water tolerance of starch-based films, when immersed into distilled water containing sodium azide, TMPyP did not significantly change their water solubility, showing an average film weight loss of 20 % after 7 days (Fig. 4A). However, the supernatant waters acquired a coloration ranging from yellowish to reddish, whose intensity at 430 nm (absorbance band can be associated to TMPyP Soret band (Kadish et al., 2010) increased with the TMPyP content in the film (Fig. 4B). This band was not evidenced for supernatant waters in which starch-based films without TMPyP were immersed. Therefore, as no disintegration of the films was observed, the films weight loss can be associated with the glycerol (Gonçalves et al., 2020) and TMPyP release from the starch-based films. When compared to the TMPyP initial amount added to each formulation, the highest TMPyP release (29 %, in relation to initial TMPyP amount, Table 1) was observed for films containing 0.25 % TMPyP, while the lowest one (19 %, Table 1) occurred for films containing 0.75 % TMPyP. Therefore, the films compaction (Fig. 2A) promoted by starch polymers, glycerol, and TMPyP intermolecular interactions minimize the TMPyP molecular interaction with water molecules and its diffusion into the surrounding aqueous media. This barrier to the lowest molecular compounds present in the starch-based network suggests that the developed biomaterials may acquire semipermeable properties similar to commercially available wound dressings (Yusof, Wee, Lim, & Khor, 2003), while offering a possibility to obtain biocompatible materials either with a fast or slow TMPyP kinetic release profile.

The TMPyP release out was also observed when starch/TMPyP-based films were put in contact with pig skin (Fig. 5). The pig skin in contact with the starch/TMPyP-based films acquired a coloration ranging from yellowish to reddish (Fig. 5A), whose colour intensity varied linearly to the TMPyP dosage. Due to the interference of the pig skin matrix, it was not possible to confirm the TMPyP permeation through the pig skin samples. The TMPyP leached out area was well noted by the films decolorization till reaching the optical characteristics of the pristine starch-based films. Fig. 5B allows to observe that the higher the TMPyP incorporated into the starch-based films, the higher was the film's weight loss percentage, increasing from 2 % to 9 %. As no TMPyP was added in the neat films, the 2 % weight loss of starch-based film can be related with the glycerol diffusion onto the skin surface. The successful TMPyP release from starch-based films to the pig skin highlighted the film's application for wound management by increasing the TMPyP concentration at the wound target site, increasing the photosensitizer efficacy during PDT (Fadel, Kassab, Abdel Fadeel, & Farag, 2020).

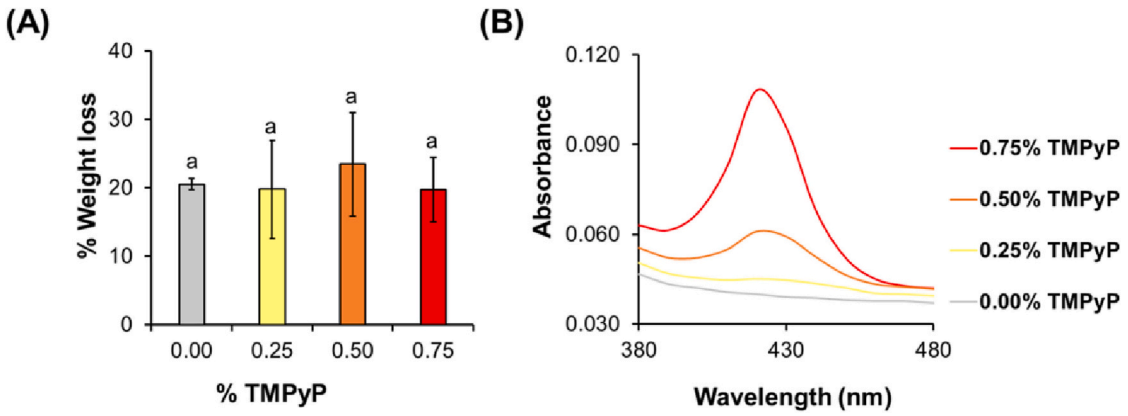

Fig. 4. Water solubility of starch- and starch/TMPyP-based films: (A) Percentage of film weight loss after immersion into distilled water containing sodium azide for 7 days and (B) UV–Visible spectra of the supernatant waters. (For statistic difference analysis, lower-case letters were used to highlight the significant differences ($p < 0.05$) between the starch- and starch/TMPyP-based films).

Table 1
Percentage of TMPyP released from starch-based films containing 0.25 % TMPyP and 0.75 % TMPyP when immersed in PBS and distilled water for 24 h.

Solvent	Sample	TMPyP release (%)
PBS	0.25 % TMPyP	99.6
	0.75 % TMPyP	97.8
Distilled water	0.25 % TMPyP	29.0
	0.75 % TMPyP	19.0

3.2. Singlet oxygen generation and antimicrobial photodynamic activity of starch/TMPyP-based films

In order to have an insight on the photodynamic efficiency of the starch/TMPyP-based films towards the Gram(−) bacterium *E. coli*, their ability to generate $^1O_2$ was first indirectly evaluated by monitoring the DPiBF absorption decay after red light irradiation for 15 min and 30 min in the presence of starch- and starch/TMPyP-based films (Fig. 6). When the neat films were irradiated with a red light (630 nm ± 20 nm) for 30 min, a decay of 14 % in the DPiBF absorption was observed, indicating that the neat starch-based films might possess some photodynamic activity. This property can be related with the presence of light-sensitive phenolic compounds derived from potato processing (Lopes et al., 2021), since the starch used in this work was obtained from potato washing slurries without any purification step. In the presence of 0.25 % TMPyP, the DPiBF absorption decreased 67 %. This $^1O_2$ production was less pronounced for films containing 0.50 % TMPyP, in which the DPiBF absorption decreased 56 % upon 30 min of irradiation with red light. This phenomenon can be related with the highest rigidity observed in starch/0.50 % TMPyP-based films and higher compaction of the polymeric network (Fig. 2). Therefore, although entrapped within the starch network, TMPyP maintained its high efficacy to generate $^1O_2$ upon irradiation.

The antimicrobial photodynamic activity of starch/TMPyP-based formulations towards an *E. coli* bioluminescent strain was evaluated using the films prepared with the lowest (0.25 %) and the highest (0.75 %) TMPyP concentrations used in this work, having the films without TMPyP as control (Fig. 7). *E. coli* was selected to perform the aPDT studies once the presence of an intricate outer membrane leads to an impermeable barrier to PS agents when compared to Gram-positive bacteria which have a porous cell wall making easier the penetration of the PS into the cell (Delcour, 2009; Pereira et al., 2014). The results had shown that, after 30 min exposed to a photodynamic treatment with white light (400–800 nm) at an irradiance of 25 mW/cm^2, in the presence of starch/TMPyP-based films, the bioluminescence of *E. coli* suffers an irradiation time-dependent decrease, indicating the loss of bacterium viability under irradiation (Fig. 7A). The photodynamic kinetic profiles were similar for all the TMPyP-based films, where the detection limit of the methodology was achieved after 15 min of irradiation, resulting in a decrease of 4.0 $\log_{10}$ (99.99 % of abundance reduction, $p < 0.05$) in the bioluminescence RLU of *E. coli*. No significant variations on the bioluminescent signal (RLU) of *E. coli* were observed (ANOVA, $p > 0.05$),

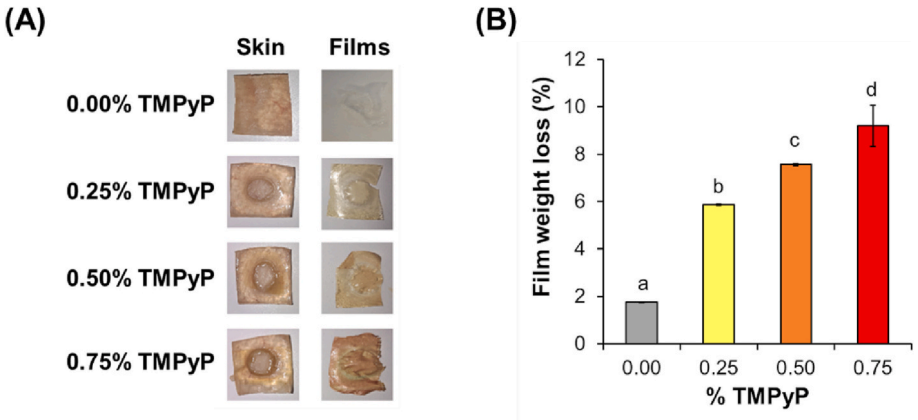

Fig. 5. TMPyP release from starch-based films to pig skin surface: (A) Visual aspect of pig skin and starch- and starch/TMPyP-based films; (B) Percentage of starch- and starch/TMPyP-based films weight loss after the contact with the pig skin surface. (For statistic difference analysis, lower-case letters were used to highlight the significant differences ($p < 0.05$) between the starch- and starch/TMPyP-based films).

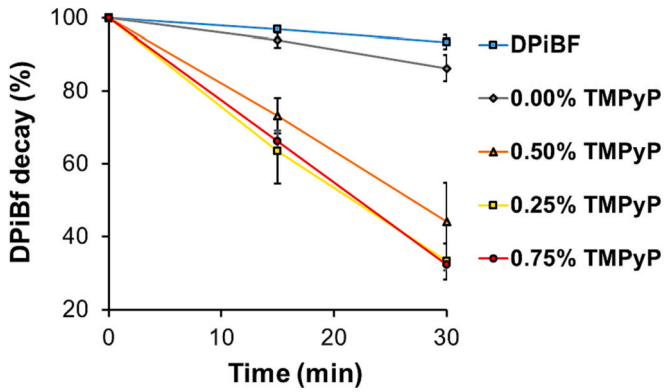

Fig. 6. Photodecomposition of DPiBF photosensitized by starch- and starch/TMPyP-based films in DMF upon irradiation with red light (630 nm ± 20 nm) at an irradiance of 14 mW/cm^2 for 15 min and 30 min.

when the starch film (with no TMPyP) was evaluated, showing that the inactivation mechanism of action was related with the TMPyP photodynamic effect.

The decrease in *E. coli* bioluminescence signal was also confirmed with the pour-plate methodology. The results obtained (Fig. 7B) confirm that both starch/TMPyP-based films loaded with the TMPyP were efficient in the photoinactivation of *E. coli*, causing a decrease of 6.0 $\log_{10}$ (99.9999 % of CFU/mL reduction, $p < 0.05$) in the viability of *E. coli* after 30 min of light irradiation. No significant differences were observed between the starch/TMPyP-based with the different concentrations of TMPyP ($p > 0.05$). The development of biocompatible starch/TMPyP-based films loaded with different amounts of the PS agent able to induce full bacteria photoinactivation is of great significance whereas permits to develop fine-tunned photoactive material without losing efficiency in the aPDT procedure. Once bacterial infections are one of the issues responsible for ineffective regenerative processes (Nesi-Reis et al., 2018), effective bacteria eradication by PS can promote enhanced wound healing mechanisms.

Experiments of TMPyP kinetic release in PBS using films containing 0.25 % and 0.75 % TMPyP (Table 1) showed that the kinetics of TMPyP release was much faster in the presence of PBS than in distilled water. This may be explained by the salting-in effect of PBS, capable of disrupting the hydrophobic interactions established between TMPyP and the starch polymeric chains. Moreover, the films washed with PBS, which retained only 2.2 % of the initial TMPyP amount, were able to inactivate *E. coli* in 60 min (Fig. 7), only 4 times slower than the time required with the non-washed starch/TMPyP-based films. The ability to control the TMPyP kinetic release with the chemical composition of the surrounding aqueous medium can be of great interest to develop wound dressings whose release of the active compound can be tuned based on the wound infection degree, allowing to improve the efficiency of the regenerative process.

3.3. *In vitro* wound healing ability of starch/TMPyP-based films

To validate the skin wound healing ability of starch- and starch/TMPyP-based films, two *in vitro* wound healing assays, with and without light irradiation, were carried out: one for mimicking the effect in skin vascularization with human microvascular endothelial cells (HMEC) and another for mimicking the skin connective tissue with human dermal fibroblasts (HDF) (Fig. 8). After the cells were confluent, a gap has created for endothelial cells (Fig. 8A, 8B) and fibroblasts (Fig. 8a, 8b) before the different treatments were applied. In 24 h, non-irradiated (Non-IR) cells were able to decrease the gap area (GA) from 100 % to 63.3 % and 4.5 % for HMEC and HMF, respectively (Figs. 8C, 8c), showing, as reported, that HDF mediates the wound closure (Tefft, Chen, & Eyckmans, 2021). When exposed to red-light, HMEC rapidly presented a GA decrease to 9.9 % (Fig. 8D), corroborating with a report that emphasizes the endothelial cells viability after irradiation with red-light LED lamp at 630 nm (Oh, Park, Lee, & Park, 2018), a similar one used in this study (red-light LED lamp at 652 nm). In turn, the applied phototherapy did not increase the HDF migration, reaching GA values like the ones observed in the non-irradiated treatment (Fig. 8c, 8d). The presence of neat starch-based films, even under dark conditions, decreased the GA for HMEC to 7.7 % (Fig. 8E), thus potentiating their migration over the wound, and HDF decreased the GA to 57.5 % (Fig. 8e). It is possible that neat starch-based films acted as a source of nutrients promoted mainly by the endothelium amylase, thus promoting HMEC migration. When red-light was irradiated during the wound healing with starch-based films, this tendency changed oppositely, being the wound closure compromised for both HMEC and HDF, reaching a GA of only 21.9 % and 26.9 %, respectively (Fig. 8F, 8f), possibly a consequence of the ROS formation that interferes with the mitochondria metabolism (Eckl et al., 2018; Sułek, Pucelik, Kobielusz, Barzowska, & Dąbrowski, 2020). Incorporating TMPyP into the starch-based films decreased the HMEC cells migration promoted by the neat films, increasing the GA values either when the wound healing was performed under dark or irradiated conditions (Figs. 8G-8J). This behavior can be related to the TMPyP release through the surround media and consequent ROS availability. When applied to HDF, the starch/TMPyP-based films promoted lower GA values than the neat films for the wound healing carried out under dark and red-light conditions (Figs. 8g-8j),

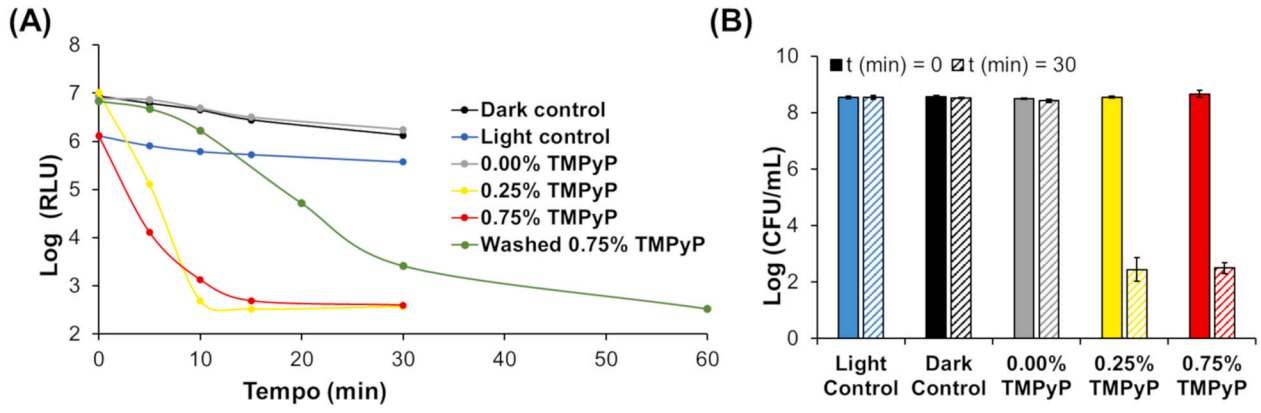

Fig. 7. Photodynamic profile of starch- and starch/TMPyP-based films for *E. coli*: (A) *E. coli* bioluminescence profile and (B) variation of colonies forming units (CFU) when exposed to starch-, starch/0.25 % TMPyP-, starch/0.75 % TMPyP-, and washed starch/0.75 % TMPyP-based films in the presence of white light at an irradiance of25 mW/cm^2 for 30 min (light dose of 45 J/cm^2). Values are presented as the mean of two independent assays with two replicates each; the standard deviation is represented by the error bars. Lines just combine experimental points.

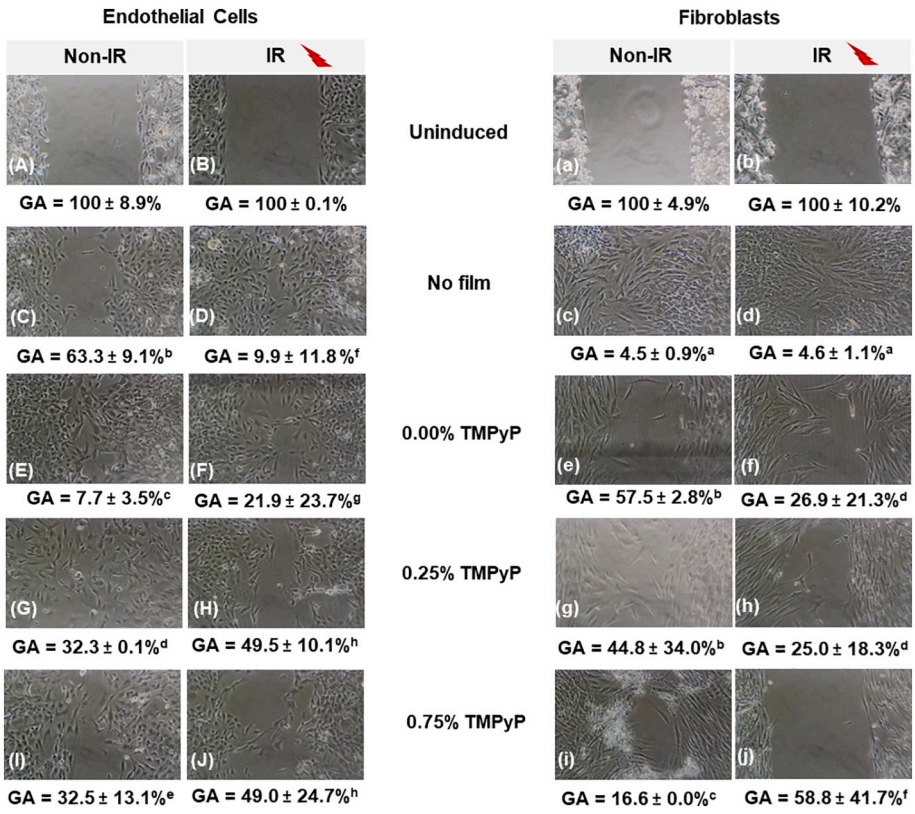

Fig. 8. Representative images of *in vitro* wound-healing assay using skin human microvascular endothelial cells (A-H, upper case letters) and human dermal fibroblasts (a-h, lower case letters). Uninduced images were the gap created at 0 h, before treatments (A, a, B, b). No film images correspond to cell migration after 24 h without starch and non-irradiated (C, c) and irradiated (D, d). After 24 h of exposure to starch- (0.00 % TMPyP) and starch/TMPyP (0.25 % TMPyP and 0.75 TMPyP)-based films, either in dark conditions or after 15 min of irradiation with red light (IR). Cellular control (no film applied) and dark control (non-irradiated, Non-IR) were used for comparison purposes. The gap area (GA) was expressed in percentage mean ± SD. The experiment was performed in triplicate. (For statistic difference analysis, lower-case letters were used to highlight the significant differences between starch- and starch/TMPyP-based films).

particularly for the films containing the highest TMPyP dosages.

As a successful wound closure requires a balanced between the slow proliferation of fibroblasts, in order to allow a proper collagen deposition and fibers orientation, and the rapid migration of endothelial cells to facilitate the skin tissue revascularization and remodeling (Barbero & Frasch, 2009), starch- and starch/TMPyP-based films revealed suitable properties to be used on active wound healing.

4. Conclusion

TMPyP conferred a yellowish/reddish coloration to starch-based films, whose intensity directly varied with the TMPyP dosage, maintaining their inherent transparency. In addition, TMPyP increased the films surface hydrophobicity and, depending on the TMPyP amount used, promoted mobility to the starch polymeric chains. Starch/TMPyP-based materials photoinactivated *E. coli* bacterium in an effective and fast way. Moreover, starch/TMPyP-based films favored the skin wound healing without requiring light. Overall, doping starch-based films with TMPyP revealed to be a promising approach to develop antimicrobial and glycocarrier biomaterials with potential to promote active and aseptic skin wound healing, opening an opportunity for extending their application to anti-infective therapies.

Abbreviations

CCR2	CC chemokine receptor 2
CCL2	CC chemokine ligand 2
CCR5	CC chemokine receptor 5
TLC	thin layer chromatography
PS	photosensitizer
aPDT	antimicrobial photodynamic therapy

CRediT authorship contribution statement

Paloma Lopes: Investigation, Methodology, Data curation, Writing – original draft. **A. Sofia M. Joaquinito:** Investigation, Methodology, Data curation, Writing – original draft. **Artur Ribeiro:** Investigation, Methodology, Data curation, Writing – review & editing. **Nuno M.M. Moura:** Conceptualization, Supervision, Validation, Writing – review & editing. **Ana T.P. Gomes:** Supervision, Writing – review & editing. **Susana G. Guerreiro:** Conceptualization, Supervision, Validation, Writing – review & editing. **M. Amparo F. Faustino:** Writing – review & editing. **Adelaide Almeida:** Writing – review & editing. **Paula Ferreira:** Writing – review & editing. **Manuel A. Coimbra:** Writing – review & editing. **M. Graça P.M.S. Neves:** Writing – review & editing. **Idalina Gonçalves:** Conceptualization, Supervision, Validation, Writing – review & editing.

Declaration of competing interest

The authors declare that they have no known competing financial interests or personal relationships that could have appeared to influence the work reported in this paper.

Data availability

No data was used for the research described in the article.

Acknowledgments

The authors thank to University of Aveiro and FCT/MCT for the financial support provided to CICECO (UIDB/50011/2020, UIDP/50011/2020, LA/P/0006/2020), LAQV-REQUIMTE (UIDB/50006/2020 and UIDP/50006/2020), CESAM (UIDP/50017/2020, UIDB/50017/2020, LA/P/0094/2020), CEB (UIDB/04469/2020), LABBELS (LA/P/0029/2020), and to projects PORP2PS (EXPL/QUI-QOR/0586/

2021) and PREVINE (FCT-PTDC/ASP-PES/29576/2017), through national funds (OE) and where applicable co-financed by the FEDER - Operational Thematic Program for Competitiveness and Internationalization - COMPETE 2020, within the PT2020 Partnership Agreement. Thanks are also due to the Portuguese NMR and Mass Networks. FCT also funded ASMJ PhD grant (2021.06854.BD), Investigator FCT program (PF, IF/00300/2015), and the Scientific Employment Stimulus program (IG, CEECIND/00430/2017; AR, 2021.02803.CEECIND). NMMM thanks FCT for funding through program DL 57/2016 (CDL-CTTRI-048-88-ARH/2018). The authors also acknowledge to POTATOPLASTIC project (POCI-01-0247-FEDER-017938), financed by FEDER through POCI, to Isolago – Indústria de Plásticos, S. A., the project leader, and to A Saloinha, Lda. company for providing the starch-rich potato washing slurries.

References

Ai, Y., & Jane, J. L. (2015). Gelatinization and rheological properties of starch. *Starch/Staerke, 67*(3–4), 213–224. https://doi.org/10.1002/star.201400201

Alves, E., Carvalho, C. M. B., Tomé, J. P. C., Faustino, M. A. F., Neves, M. G. P. M. S., Tomé, A. C., Cavaleiro, J. A. S., Cunha, Â., Mendo, S., & Almeida, A. (2008). Photodynamic inactivation of recombinant bioluminescent Escherichia coli by cationic porphyrins under artificial and solar irradiation. *Journal of Industrial Microbiology and Biotechnology, 35*(11), 1447–1454. https://doi.org/10.1007/s10295-008-0446-2

Alves, E., Rodrigues, J. M. M., Faustino, M. A. F., Neves, M. G. P. M. S., Cavaleiro, J. A. S., Lin, Z., Cunha, Â., Nadais, M. H., Tomé, J. P. C., & Almeida, A. (2014). A new insight on nanomagnet–porphyrin hybrids for photodynamic inactivation of microorganisms. *Dyes and Pigments, 110*, 80–88. https://doi.org/10.1016/J.DYEPIG.2014.05.016

Andreu, V., Mendoza, G., Arruebo, M., & Irusta, S. (2015). Smart dressings based on nanostructured fibers containing natural origin antimicrobial, anti-inflammatory, and regenerative compounds. *Materials, 8*(8), 5154–5193. https://doi.org/10.3390/ma8085154

Barbero, A. M., & Frasch, H. F. (2009). Pig and guinea pig skin as surrogates for human in vitro penetration studies: A quantitative review. Issue 1. In , *Toxicol In Vitro: Vol. 23. Toxicology in Vitro* (pp. 1–13). https://doi.org/10.1016/j.tiv.2008.10.008.

Basiak, E., Lenart, A., & Debeaufort, F. (2018). How glycerol and water contents affect the structural and functional properties of starch-based edible films. *Polymers, 10*(4), 412. https://doi.org/10.3390/polym10040412

Berg, K., Selbo, P. K., Weyergang, A., Dietze, A., Prasmickaite, L., Bonsted, A., Engesaeter, B., Angell-Petersen, E., Warloe, T., Frandsen, N., & Høgset, A. (2005). Porphyrin-related photosensitizers for cancer imaging and therapeutic applications. *Journal of Microscopy, 218*(2), 133–147. https://doi.org/10.1111/j.1365-2818.2005.01471.x

Bertoft, E. (2017). Understanding starch structure: recent progress. *Agronomy, 7*(3), 56. https://doi.org/10.3390/agronomy7030056

Carvalho, C. M. B., Alves, E., Costa, L., Tomé, J. P. C., Faustino, M. A. F., Neves, M. G. P. M. S., Tomé, A. C., Cavaleiro, J. A. S., Almeida, A., Cunha, Â., Lin, Z., & Rocha, J. (2010). Functional cationic nanomagnet - Porphyrin hybrids for the photoinactivation of microorganisms. *ACS Nano, 4*(12), 7133–7140. https://doi.org/10.1021/nn1026092

Costa, L., Tomé, J. P. C., Neves, M. G. P. M. S., Tomé, A. C., Cavaleiro, J. A. S., Faustino, M. A. F., Cunha, Â., Gomes, N. C. M., & Almeida, A. (2011). Evaluation of resistance development and viability recovery by a non-enveloped virus after repeated cycles of aPDT. *Antiviral Research, 91*(3), 278–282. https://doi.org/10.1016/j.antiviral.2011.06.007

Das, A., Uppaluri, R., & Das, C. (2019). Feasibility of poly-vinyl alcohol/starch/glycerol/citric acid composite films for wound dressing applications. *International Journal of Biological Macromolecules, 131*, 998–1007. https://doi.org/10.1016/j.ijbiomac.2019.03.160

Delcour, A. H. (2009). Outer membrane permeability and antibiotic resistance. *Biochimica et Biophysica Acta (BBA) - Proteins and Proteomics, 1794*(5), 808–816. https://doi.org/10.1016/j.bbapap.2008.11.005

Eckl, D. B., Dengler, L., Nemmert, M., Eichner, A., Bäumler, W., & Huber, H. (2018). A closer look at dark toxicity of the photosensitizer TMPyP in bacteria. *Photochemistry and Photobiology, 94*(1), 165–172. https://doi.org/10.1111/PHP.12846

Eskandarinia, A., Kefayat, A., Rafienia, M., Agheb, M., Navid, S., & Ebrahimpour, K. (2019). Cornstarch-based wound dressing incorporated with hyaluronic acid and propolis: In vitro and in vivo studies. *Carbohydrate Polymers, 216*, 25–35. https://doi.org/10.1016/j.carbpol.2019.03.091

Fadel, M., Kassab, K., Abdel Fadeel, D. A., & Farag, M. A. (2020). Topical photodynamic therapy of tumor bearing mice with meso-tetrakis (N-methyl-4-pyridyl) porphyrin loaded in ethosomes. *Photodiagnosis and Photodynamic Therapy, 30*, Article 101789. https://doi.org/10.1016/j.pdpdt.2020.101789

Feng, M., Yu, L., Zhu, P., Zhou, X., Liu, H., Yang, Y., Zhou, J., Gao, C., Bao, X., & Chen, P. (2018). Development and preparation of active starch films carrying tea polyphenol. *Carbohydrate Polymers, 196*, 162–167. https://doi.org/10.1016/j.carbpol.2018.05.043

Ferreira, H., & Ribeiro, A. (2015). Deformable liposomes for the transdermal delivery of piroxicam. *Journal of Pharmaceutics & Drug Delivery Research, 04*(04). https://doi.org/10.4172/2325-9604.1000139

Gomes, A. T. P. C., Neves, M. G. P. M. S., & Cavaleiro, J. A. S. (2018). Cancer, photodynamic therapy and porphyrin-type derivatives. *Anais Da Academia Brasileira de Ciencias, 90*(1), 993–1026. https://doi.org/10.1590/0001-3765201820170811

Gonçalves, I., Hernández, D., Cruz, C., Lopes, J., Barra, A., Nunes, C., da Silva, J. A. L., Ferreira, P., & Coimbra, M. A. (2021). Relevance of genipin networking on rheological, physical, and mechanical properties of starch-based formulations. *Carbohydrate Polymers, 254*, Article 117236. https://doi.org/10.1016/j.carbpol.2020.117236

Gonçalves, I., Lopes, J., Barra, A., Hernández, D., Nunes, C., Kapusniak, K., Kapusniak, J., Evtyugin, D. V., Lopes da Silva, J. A., Ferreira, P., & Coimbra, M. A. (2020). Tailoring the surface properties and flexibility of starch-based films using oil and waxes recovered from potato chips byproducts. *International Journal of Biological Macromolecules, 163*, 251–259. https://doi.org/10.1016/j.ijbiomac.2020.06.231

Gupta, B., Agarwal, R., & Alam, M. S. (2010). Textile-based smart wound dressings. *Indian Journal of Fibre and Textile Research, 35*(2), 174–187.

Hanakova, A., Bogdanova, K., Tomankova, K., Pizova, K., Malohlava, J., Binder, S., Bajgar, R., Langova, K., Kolar, M., Mosinger, J., & Kolarova, H. (2014). The application of antimicrobial photodynamic therapy on S. aureus and E. coli using porphyrin photosensitizers bound to cyclodextrin. *Microbiological Research, 169*(2–3), 163–170. https://doi.org/10.1016/j.micres.2013.07.005

Hassan, A., Niazi, M. B. K., Hussain, A., Farrukh, S., & Ahmad, T. (2018). Development of anti-bacterial PVA/starch based hydrogel membrane for wound dressing. *Journal of Polymers and the Environment, 26*(1), 235–243. https://doi.org/10.1007/s10924-017-0944-2

Hemamalini, T., & Giri Dev, V. R. (2018). Comprehensive review on electrospinning of starch polymer for biomedical applications. *International Journal of Biological Macromolecules, 106*, 712–718. https://doi.org/10.1016/j.ijbiomac.2017.08.079

Jiang, L., Gan, C. R. R., Gao, J., & Loh, X. J. (2016). A perspective on the trends and challenges facing porphyrin-based anti-microbial materials. *Small, 12*(27), 3609–3644. https://doi.org/10.1002/smll.201600327

Jukola, H., Nikkola, L., Gomes, M. E., Reis, R. L., & Ashammakhi, N. (2008). Electrospun starch-polycaprolactone nanofiber-based constructs for tissue engineering. *AIP Conference Proceedings, 973*(1), 971. https://doi.org/10.1063/1.2896914

Kadish, K. M., Smith, K. M., & Guilard, R. (2010). In K. M. Kadish, K. M. Smith, & R. Guilard (Eds.), *Handbook of porphyrin science with applications to chemistry, physics, materials science, engineering, biology and medicine.* World Scientific Publishing Company Co.

Kuorwel, K., Cran, M. J., Sonneveld, K., Miltz, J., & Bigger, S. W. (2011). Antimicrobial activity of natural agents coated on starch-based films against Staphylococcus aureus. *Journal of Food Science, 76*(8), M531–M537. https://doi.org/10.1111/j.1750-3841.2011.02344.x

Kuzmin, S. M., Chulovskaya, S. A., & Parfenyuk, V. I. (2018). Structures and properties of porphyrin-based film materials part I. The films obtained via vapor-assisted methods. *Advances in Colloid and Interface Science, 253*, 23–34. https://doi.org/10.1016/j.cis.2018.02.001

Kwiatkowski, S., Knap, B., Przystupski, D., Saczko, J., Kędzierska, E., Knap-Czop, K., Kotlińska, J., Michel, O., Kotowski, K., & Kulbacka, J. (2018). Photodynamic therapy – Mechanisms, photosensitizers and combinations. *Biomedicine & Pharmacotherapy, 106*, 1098–1107. https://doi.org/10.1016/j.biopha.2018.07.049

Lancuški, A., Abu Ammar, A., Avrahami, R., Vilensky, R., Vasilyev, G., & Zussman, E. (2017). Design of starch-formate compound fibers as encapsulation platform for biotherapeutics. *Carbohydrate Polymers, 158*, 68–76. https://doi.org/10.1016/j.carbpol.2016.12.003

Laohakunjit, N., & Noomhorm, A. (2004). Effect of plasticizers on mechanical and barrier properties of rice starch film. *Starch/Staerke, 56*(8), 348–356. https://doi.org/10.1002/star.200300249

Liang, J., & Ludescher, R. D. (2015). Effects of glycerol on the molecular mobility and hydrogen bond network in starch matrix. *Carbohydrate Polymers, 115*, 401–407. https://doi.org/10.1016/j.carbpol.2014.08.105

Liang, Y., He, J., & Guo, B. (2021). Functional hydrogels as wound dressing to enhance wound healing. *ACS Nano, 15*, 12687–12722. https://doi.org/10.1021/acsnano.1c04206

Liu, H., Xie, F., Yu, L., Chen, L., & Li, L. (2009). Thermal processing of starch-based polymers. *Progress in Polymer Science (Oxford), 34*(12), 1348–1368. https://doi.org/10.1016/j.progpolymsci.2009.07.001

Lopes, J., Gonçalves, I., Nunes, C., Teixeira, B., Mendes, R., Ferreira, P., & Coimbra, M. A. (2021). Potato peel phenolics as additives for developing active starch-based films with potential to pack smoked fish fillets. *Food Packaging and Shelf Life, 28*(April), Article 100644. https://doi.org/10.1016/j.fpsl.2021.100644

Mesquita, M. Q., Dias, C. J., Gamelas, S., Fardilha, M., Neves, M. G. P. M. S., & Faustino, M. A. F. (2018). An insight on the role of photosensitizer nanocarriers for photodynamic therapy. *Anais Da Academia Brasileira de Ciencias, 90*(1), 1101–1130. https://doi.org/10.1590/0001-3765201720170800

Mesquita, M. Q., Dias, C. J., Neves, M. G. P. M. S., Almeida, A., & Faustino, M. A. F. (2018). Revisiting current photoactive materials for antimicrobial photodynamic therapy. *Molecules, 23*(10), 2424. https://doi.org/10.3390/MOLECULES23102424

Mesquita, M. Q., Menezes, J. C. J. M. D. S., Pires, S. M. G., Neves, M. G. P. M. S., Simões, M. M. Q., & Tomé, A. C. (2014). Pyrrolidine-fused chlorin photosensitizer immobilized on solid supports for the photoinactivation of gram negative bacteria. *Dyes and Pigments, 110*, 123–133. https://doi.org/10.1016/J.DYEPIG.2014.04.025

Mogoşanu, G. D., & Grumezescu, A. M. (2014). Natural and synthetic polymers for wounds and burns dressing. *International Journal of Pharmaceutics, 463*(2), 127–136. https://doi.org/10.1016/j.ijpharm.2013.12.015

Moreno, O., Atarés, L., & Chiralt, A. (2015). Effect of the incorporation of antimicrobial/antioxidant proteins on the properties of potato starch films. *Carbohydrate Polymers, 133*, 353–364. https://doi.org/10.1016/j.carbpol.2015.07.047

Nesi-Reis, V., Lera-Nonose, D. S. S. L., Oyama, J., Silva-Lalucci, M. P. P., Demarchi, I. G., Aristides, S. M. A., Teixeira, J. J. V., Silveira, T. G. V., & Lonardoni, M. V. C. (2018). Contribution of photodynamic therapy in wound healing: A systematic review. *Photodiagnosis and Photodynamic Therapy, 21*, 294–305. https://doi.org/10.1016/j.pdpdt.2017.12.015

Nunes, C., Maricato, É., Cunha, Â., Nunes, A., da Silva, J. A. L., & Coimbra, M. A. (2013). Chitosan–caffeic acid–genipin films presenting enhanced antioxidant activity and stability in acidic media. *Carbohydrate Polymers, 91*(1), 236–243. https://doi.org/10.1016/j.carbpol.2012.08.033

Nyman, E. S., & Hynninen, P. H. (2004). Research advances in the use of tetrapyrrolic photosensitizers for photodynamic therapy. *Journal of Photochemistry and Photobiology B: Biology, 73*(1–2), 1–28. https://doi.org/10.1016/j.jphotobiol.2003.10.002

O'Connor, A. E., Gallagher, W. M., & Byrne, A. T. (2009). Porphyrin and nonporphyrin photosensitizers in oncology: Preclinical and clinical advances in photodynamic therapy. *Photochemistry and Photobiology, 85*(5), 1053–1074. https://doi.org/10.1111/j.1751-1097.2009.00585.x

Oh, K. J., Park, J., Lee, H. S., & Park, K. (2018). Effects of light-emitting diodes irradiation on human vascular endothelial cells. *International Journal of Impotence Research, 30*(6), 312–317. https://doi.org/10.1038/s41443-018-0051-5

Ouitas, N. A., & Heard, C. M. (2009). A novel ex vivo skin model for the assessment of the potential transcutaneous anti-inflammatory effect of topically applied Harpagophytum procumbens extract. *International Journal of Pharmaceutics, 376*(1–2), 63–68. https://doi.org/10.1016/j.ijpharm.2009.04.017

Pal, K., Banthia, A. K., & Majumdar, D. K. (2006). Preparation of transparent starch based hydrogel membrane with potential application as wound dressing. *Trends in Biomaterials and Artificial Organs, 20*(1), 59–67.

Pereira, M. A., Faustino, M. A. F., Tomé, J. P. C., Neves, M. G. P. M. S., Tomé, A. C., Cavaleiro, J. A. S., Cunha, Â., & Almeida, A. (2014). Influence of external bacterial structures on the efficiency of photodynamic inactivation by a cationic porphyrin. *Photochemical and Photobiological Sciences, 13*(4), 680–690. https://doi.org/10.1039/C3PP50408E

Pyla, R., Kim, T. J., Silva, J. L., & Jung, Y. S. (2010). Enhanced antimicrobial activity of starch-based film impregnated with thermally processed tannic acid, a strong antioxidant. *International Journal of Food Microbiology, 137*(2–3), 154–160. https://doi.org/10.1016/j.ijfoodmicro.2009.12.011

Ruhl, C. M., Urbancic, J. H., Foresman, P. A., Cox, M. J., Rodeheaver, G. T., Zura, R. D., & Edlich, R. F. (1994). A new hazard of cornstarch, an absorbable dusting powder. *The Journal of Emergency Medicine, 12*(1), 11–14. https://doi.org/10.1016/0736-4679(94)90004-3

Simões, C., Gomes, M. C., Neves, M. G. P. M. S., Cunha, Â., Tomé, J. P. C., Tomé, A. C., Cavaleiro, J. A. S., Almeida, A., & Faustino, M. A. F. (2016). Photodynamic inactivation of Escherichia coli with cationic meso-tetraarylporphyrins – The charge number and charge distribution effects. *Catalysis Today, 266*, 197–204. https://doi.org/10.1016/J.CATTOD.2015.07.031

Simões, D., Miguel, S. P., Ribeiro, M. P., Coutinho, P., Mendonça, A. G., & Correia, I. J. (2018). Recent advances on antimicrobial wound dressing: A review. *European Journal of Pharmaceutics and Biopharmaceutics, 127*, 130–141. https://doi.org/10.1016/j.ejpb.2018.02.022

Spiller, W., Kliesch, H., Wöhrle, D., Hackbarth, S., Röder, B., & Schnurpfeil, G. (1998). Singlet oxygen quantum yields of different photo-sensitizers in polar solvents and micellar solutions. *Journal of Porphyrins and Phthalocyanines, 2*(2), 145–158. https://doi.org/10.1002/(SICI)1099-1409(199803/04)2:2<145::AID-JPP60>3.0.CO;2-2

Sułek, A., Pucelik, B., Kobielusz, M., Barzowska, A., & Dąbrowski, J. M. (2020). Photodynamic inactivation of bacteria with porphyrin derivatives: Effect of charge, lipophilicity, ROS generation, and cellular uptake on their biological activity in vitro. *International Journal of Molecular Sciences, 21*(22), 8716. https://doi.org/10.3390/IJMS21228716

Sunthornvarabhas, J., Chatakanonda, P., Piyachomkwan, K., & Sriroth, K. (2011). Electrospun polylactic acid and cassava starch fiber by conjugated solvent technique. *Materials Letters, 65*(6), 985–987. https://doi.org/10.1016/J.MATLET.2010.12.038

Tavares, A., Carvalho, C. M. B., Faustino, M. A., Neves, M. G. P. M. S., Tomé, J. P. C., Tomé, A. C., Cavaleiro, J. A. S., Cunha, Â., Gomes, N. C. M., Alves, E., & Almeida, A. (2010). Antimicrobial photodynamic therapy: Study of bacterial recovery viability and potential development of resistance after treatment. *Marine Drugs, 8*(1), 91–105. https://doi.org/10.3390/MD8010091

Tefft, J. B., Chen, C. S., & Eyckmans, J. (2021). Reconstituting the dynamics of endothelial cells and fibroblasts in wound closure. *APL Bioengineering, 5*(1), Article 016102. https://doi.org/10.1063/5.0028651

Thakur, R., Pristijono, P., Golding, J. B., Stathopoulos, C. E., Scarlett, C., Bowyer, M., Singh, S. P., & Vuong, Q. V. (2018). Effect of starch physiology, gelatinization, and retrogradation on the attributes of rice starch-ι-carrageenan film. *Starch - Stärke, 70*, Article 1700099. https://doi.org/10.1002/star.201700099

Torres, F. G., Commeaux, S., & Troncoso, O. P. (2013). Starch-based biomaterials for wound-dressing applications. *Starch/Staerke, 65*(7–8), 543–551. https://doi.org/10.1002/star.201200259

Tottoli, E. M., Dorati, R., Genta, I., Chiesa, E., Pisani, S., & Conti, B. (2020). Skin wound healing process and new emerging technologies for skin wound care and regeneration. *Pharmaceutics, 12*(8), 735. https://doi.org/10.3390/pharmaceutics12080735

Vallejo, M. C. S., Moura, N. M. M., Faustino, M. A. F., Almeida, A., Gonçalves, I., Serra, V. V., & Neves, M. G. P. M. S. (2021). An insight into the role of non-porphyrinoid photosensitizers for skin wound healing. *International Journal of Molecular Sciences, 22*(1), 234. https://doi.org/10.3390/ijms22010234

Vallejo, M. C. S., Moura, N. M. M., Gomes, A. T. P. C., Joaquinito, A. S. M., Faustino, M. A. F., Almeida, A., Gonçalves, I., Serra, V. V., & Neves, M. G. P. M. S. (2021). The role of porphyrinoid photosensitizers for skin wound healing. *International Journal of Molecular Sciences, 22*(8), 4121. https://doi.org/10.3390/ijms22084121

Vallejo, M. C. S., Reis, M. J. A., Pereira, A. M. V. M., Serra, V. V., Cavaleiro, J. A. S., Moura, N. M. M., & Neves, M. G. P. M. S. (2021). Merging pyridine(s) with porphyrins and analogues: An overview of synthetic approaches. *Dyes and Pigments, 191*, Article 109298. https://doi.org/10.1016/j.dyepig.2021.109298

Vieira, C., Gomes, A. T. P. C., Mesquita, M. Q., Moura, N. M. M., Neves, M. G. P. M. S., Faustino, M. A. F., & Almeida, A. (2018). An insight into the potentiation effect of potassium iodide on aPDT efficacy. *Frontiers in Microbiology, 9*, 2665. https://doi.org/10.3389/fmicb.2018.02665

Wang, H., Wang, W., Jiang, S., Jiang, S., Zhai, L., & Jiang, Q. (2011). Poly(vinyl alcohol)/oxidized starch fibres via electrospinning technique: Fabrication and characterization. *Iranian Polymer Journal (English Edition), 20*(7), 551–558.

Wang, S., Li, C., Copeland, L., Niu, Q., & Wang, S. (2015). Starch retrogradation: A comprehensive review. *Comprehensive Reviews in Food Science and Food Safety, 14*(5), 568–585. https://doi.org/10.1111/1541-4337.12143

Wang, W., Jin, X., Zhu, Y., Zhu, C., Yang, J., Wang, H., & Lin, T. (2016). Effect of vapor-phase glutaraldehyde crosslinking on electrospun starch fibers. *Carbohydrate Polymers, 140*, 356–361. https://doi.org/10.1016/j.carbpol.2015.12.061

Yusof, N. L. B. M., Wee, A., Lim, L. Y., & Khor, E. (2003). Flexible chitin films as potential wound-dressing materials: Wound model studies. *Journal of Biomedical Materials Research, 66A*, 224–232. https://doi.org/10.1002/jbm.a.10545

Zarrintaj, P., Moghaddam, A. S., Manouchehri, S., Atoufi, Z., Amiri, A., Amirkhani, M. A., Nilforoushzadeh, M. A., Saeb, M. R., Hamblin, M. R., & Mozafari, M. (2017). Can regenerative medicine and nanotechnology combine to heal wounds? The search for the ideal wound dressing. *Nanomedicine, 12*(19), 2403–2422. https://doi.org/10.2217/nnm-2017-0173

Zeng, R., Lin, C., Lin, Z., Chen, H., Lu, W., Lin, C., & Li, H. (2018). Approaches to cutaneous wound healing: Basics and future directions. *Cell and Tissue Research, 374*(2), 217–232. https://doi.org/10.1007/s00441-018-2830-1

Zhai, M., Yoshii, F., Kume, T., & Hashim, K. (2002). Syntheses of PVA/starch grafted hydrogels by irradiation. *Carbohydrate Polymers, 50*(3), 295–303. https://doi.org/10.1016/S0144-8617(02)00031-0

Zhang, J., Jiang, C., Figueiró Longo, J. P., Azevedo, R. B., Zhang, H., & Muehlmann, L. A. (2018). An updated overview on the development of new photosensitizers for anticancer photodynamic therapy. *Acta Pharmaceutica Sinica B, 8*(2), 137–146. https://doi.org/10.1016/j.apsb.2017.09.003

Zhong, S. P., Zhang, Y. Z., & Lim, C. T. (2010). Tissue scaffolds for skin wound healing and dermal reconstruction. *Wiley Interdisciplinary Reviews: Nanomedicine and Nanobiotechnology, 2*(5), 510–525. https://doi.org/10.1002/wnan.100

Zhu, F., & Xie, Q. (2018). Structure and physicochemical properties of starch. In , *1. Physical modifications of starch* (pp. 1–14). https://doi.org/10.1007/978-981-13-0725-6_1